JOC Article
pubs.acs.org/joc

Catalytic Role of Vicinal OH in Ester Aminolysis: Proton Shuttle versus Hydrogen Bond Stabilization

Miroslav A. Rangelov,*[,†] Galina P. Petrova,[‡] Vihra M. Yomtova,[†] and Georgi N. Vayssilov*[,‡]

[†]*Laboratory of BioCatalysis, Institute of Organic Chemistry, Bulgarian Academy of Sciences, Str. Acad. G. Bontchev, Bl. 9, 1113 Sofia, Bulgaria, and* [‡]*Faculty of Chemistry, University of Sofia, Boulevard James Bouchier 1, 1164 Sofia, Bulgaria*

mran@orgchm.bas.bg; gnv@chem.uni-sofia.bg.

Received May 18, 2010

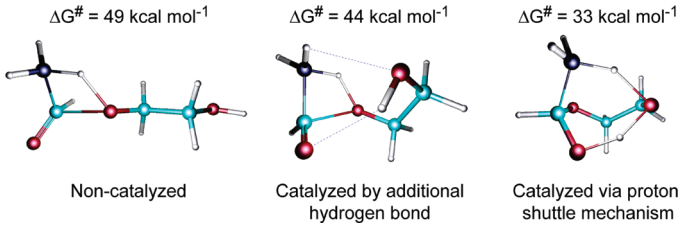

This computational study provoked by the process of peptide bond formation in the ribosome investigates the influence of the vicinal OH group in monoacylated diols on the elementary acts of ester aminolysis. Two alternative approaches for this influence on ester ammonolysis were considered: stabilization of the transition states by hydrogen bonds and participation of the vicinal hydroxyl in proton transfer (proton shuttle). The activation due to hydrogen bonds of the vicinal hydroxyl via tetragonal transition states was rather modest; the free energy of activation was reduced by only 5.2 kcal/mol compared to the noncatalyzed reaction. The catalytic activation via the proton shuttle mechanism with participation of the vicinal OH in the proton transfer via hexagonal transition states resulted in considerable reduction of the free energy of activation to 33.5 kcal/mol, i.e., 16.0 kcal/mol lower than in the referent process. Accounting for the influence of the environment on the reaction center by a continuum model (for ε from 5 to 80) resulted in further stabilization of the rate-determining transition state by 4−5 kcal/mol. The overall reduction of the reaction barrier by about 16 kcal/mol as compared to the noncatalyzed process corresponds to about 10^9-fold acceleration of the reaction, in agreement with the experimental estimate for acceleration of this process in the ribosome.

Introduction

The elementary chemical reaction leading to peptide bond synthesis in the ribosome is an aminolysis reaction. During the elementary act of peptide bond formation the growing polypeptide chain, esterified to the *cis*-1,2-diol of tRNA 3′-terminal adenosine, reacts with the next amino acid in the ribosome peptidyl transfer center. For this reason, the aminolysis of esters was extensively studied both experimentally[1] and theoretically[2] as a model reaction for the formation of peptide bonds in living cells. Various computational studies on the mechanism of this reaction were based on small model systems. In order to simulate the ribosome interior at the peptidyl transferase center,[3] these model studies are performed under vacuum or in aprotic solvents with low polarity. Thus, the reaction occurs without

(1) (a) Rodnina, M. V.; Beringer, M.; Wintermeyer, W. *Q. Rev. Biophys.* **2006**, *39*, 203–225. (b) Zhong, M. H.; Strobel, S. A. *J. Org. Chem.* **2008**, *73*, 603–611. (c) Simonovic, M.; Steitz, T. A. *Proc. Natl. Acad. Sci. U. S. A.* **2008**, *105*, 500–505. (d) Schroeder, G. K.; Wolfenden, R. *Biochemistry* **2007**, *46*, 4037–4044. (e) Weinger, J. S.; Parnell, K. M.; Dorner, S.; Green, R.; Strobel, S. A. *Nat. Struct. Mol. Biol.* **2004**, *11*, 1101–1106. (f) Dorner, S.; Panuschka, C.; Schmid, W.; Barta, A. *Nucleic Acids Res.* **2003**, *31*, 6536–6542.

(2) (a) Strajbl, M.; Florian, J.; Warshel, A. *J. Am. Chem. Soc.* **2000**, *122*, 5354–5366. (b) Trobro, S.; Åqvist, J. *Proc. Natl. Acad. Sci. U. S. A.* **2005**, *102*, 12395–12400. (c) Trobro, S.; Aqvist, J. *Biochemistry* **2006**, *45*, 7049–7056. (d) Gindulyte, A.; Bashan, A.; Agmon, I.; Massa, L.; Yonath, A.; Karel, J. *Proc. Natl. Acad. Sci. U. S. A.* **2006**, *103*, 13327–13332.

(3) Ban, N.; Nissen, P.; Hansen, J.; Moore, P. B.; Steitz, T. A. *Science* **2000**, *289*, 905–920.

Published on Web 09/15/2010 DOI: 10.1021/jo100886p

formation of zwitterionic intermediates, typical for reactions taking place in water[4] or in strongly polar enzyme environments.[5] Several groups[6,7] investigated peptide bond formation in formamide from ammonia and formic acid and proposed two reaction pathways, concerted and stepwise, that have comparable reaction barriers or with small preference of one of the reaction mechanisms. Galabov et al.[7] found that accounting for the solvent effect (acetonitrile) via the polarizable continuum model (PCM) reduced the activation barrier of the concerted mechanism as compared to the stepwise one. On the other hand, for larger model reactants such as methylformate, methylacetate, methylamine, etc.,[6d,7a,c] the preference for a concerted or stepwise mechanism depends on the reactants. All these model studies, however, suggested that the activation barrier of the (uncatalyzed) process is typically above 40 kcal/mol, which corresponds to a rather low reaction rate incomparable with the actual reaction rates of peptide bond formation in living cells.

In order to clarify the reasons for the relatively high reaction rate, the catalytic effect of external molecules (e.g., water, ammonia, or larger molecules having both proton-donating and proton-accepting centers) has been modeled.[8−10] Indeed, these external molecules were found to reduce the activation barrier by facilitation of the proton transfer in the reaction center. Although, the XRD studies[3] have hypothesized that water may be present in the ribosome interior, the participation of an occasionally appearing water molecule at the reaction center in the formation of each individual peptide bond cannot be considered as a reliable option. Such water molecules may also cause hydrolysis of the growing peptide chain from the tRNA instead of catalyzing each aminolysis step. An alternative catalytic effect on the reaction could come from the 2′-OH of the 3′ terminal adenosine of tRNA, which is always close to the reaction center. The crucial role of the vicinal 2′-OH on the catalytic activity of ribozymes was experimentally confirmed by the loss of peptidyl transferase activity of the ribosome with mutant 2′-deoxy-peptidyl-tRNA.[1e,11] Thus, despite the remarkable progress in ribosome structure investigations, the mechanism of peptide bond formation in the ribosome remains obscure. In our earlier work we modeled the intramolecular catalytic effect of the vicinal OH group by the ammonolysis of monoacylated catechol.[12] In that case the vicinal OH stabilizes the transition states of the reaction via formation of hydrogen bonds (HB) with reaction centers, but the estimated reduction of the activation energy with respect to a substrate without a vicinal OH group was found to be rather small, 2.2 kcal/mol. Thus, in order to elucidate the influence of the vicinal hydroxyl group, here we investigate its influence within a more flexible diol model, 1-*O*-formyl-1,2-ethanediol. This substrate is suitable as a model since the vicinal hydroxyls are bound to two neighboring sp^3-hybridized carbon atoms, similarly to the 3′- and 2′-OH of tRNA in the 3′ terminal adenosine. In a preliminary communication,[13] we reported considerable reduction of the activation barrier of the whole process due to participation of the vicinal hydroxyl in the proton transfer cycle. Here, we report the detailed results of the investigation including an exhaustive search for various possible conformations of the transition states in which the vicinal hydroxyl group forms intramolecular hydrogen bonds resulting in stabilization of the observed structures or actively participates in the proton transfer, the so-called proton shuttle mechanism. In addition, we determined the optimal positions of an adjacent OH group for lowering the energy of different transition states via formation of hydrogen bonds.

A recent paper by Wallin and Åqvist[14] extended the idea of participation of the vicinal OH in the proton transfer to inclusion of one or two additional water molecules in the transition state, thus forming at least three fused rings (seven- and eight-membered) in which bond formation and breaking occur. The reduction of the activation enthalpy of the reaction to 18 kcal/mol, although fitting well the experimental estimate,[15] should be taken with caution due to neglect of the entropic contribution caused by the frustrated mobility of the water molecules.

Results and Discussion

Various theoretical studies[2,6−10] have established that the noncatalyzed ammonolysis of esters in aprotic media occurs via either a concerted or a stepwise mechanism, shown in the left-hand side of Scheme 1a (for the notation applied see Scheme 1b). The structure of the transition states of both mechanisms is similar: tetragonal formed by C, O, N/O, and H atoms located almost in one plane. The concerted mechanism proceeds in a single step via the transition state TSc[4] and involves nucleophilic attack of the N atom to the carbonyl carbon atom, simultaneous proton transfer from ammonia to the substrate molecule, and a cleavage of the ester C−Oe bond, leading to formation of the products. On the other hand, the stepwise mechanism goes through formation of an intermediate, I, in which the NH_3 molecule is attached to the C=O bond of the ester and the former carbonyl carbon atom is in a tetrahedral configuration. The transition states for formation and decomposition of this intermediate, TS1 and TS2, include active participation of the carbonyl Oc atom in the process via subsequent addition of ammonia and elimination of alcohol.

(4) (a) Chalmet, S.; Harb, W.; Ruiz-Lopez, M. F. *J. Phys. Chem. A* **2001**, *105*, 11574–11581. (b) Sung, D. D.; Koo, I. S.; Yang, K.; Lee, I. *Chem. Phys. Lett.* **2006**, *426*, 280–284.

(5) Perdih, A.; Hodoscek, M.; Solmajer, T. *Proteins* **2009**, *74*, 744–759.

(6) (a) Oie, T.; Loew, G. H.; Burt, S. K.; Binkley, J. S.; MacElroy, R. D. *J. Am. Chem. Soc.* **1982**, *104*, 6169–6174. (b) Jensen, J. H.; Baldridge, K. K.; Gordon, M. S. *J. Phys. Chem.* **1992**, *96*, 8340–8351. (c) Wang, L.; Zipse, H. *Liebigs Ann.* **1996**, 1501–2509. (d) Zipse, H.; Wang, L.; Houk, K. N. *Liebigs Ann.* **1996**, 1511–1522.

(7) (a) Ilieva, S.; Galabov, B.; Musaev, D. G.; Morokuma, K.; Schaefer, H. F., III. *J. Org. Chem.* **2003**, *68*, 1496–1502. (b) Galabov, B.; Atanasov, Y.; Ilieva, S.; Schaefer, H. F., III. *J. Phys. Chem. A* **2005**, *109*, 11470–11474. (c) Galabov, B.; Ilieva, S.; Hadjieva, B.; Atanasov, Y.; Schaefer, H. F., III. *J. Phys. Chem. A* **2008**, *112*, 6700–6707.

(8) (a) Oie, T.; Loew, G. H.; Burt, S. K.; MacElroy, R. D. *J. Am. Chem. Soc.* **1983**, *105*, 2221–2227. (b) Williams, I. H. *J. Am. Chem. Soc.* **1987**, *109*, 6299–6307. (c) Strajbl, M.; Florian, J.; Warshel, A. *J. Phys. Chem. B* **2001**, *105*, 4471–4484. (d) Sharma, P. K.; Xiang, Y.; Kato, M.; Warshel, A. *Biochemistry* **2005**, *44*, 11307–11314.

(9) Yang, W.; Drueckhammer, D. G. *Org. Lett.* **2000**, *2*, 4133–4136.

(10) Jin, L.; Wu, Y.; Kim, C. K.; Xue, Y. *J. Mol. Struct.* (*THEOCHEM*) **2010**, *942*, 137–144.

(11) Changalov, M. M.; Ivanova, G. D.; Rangelov, M. A.; Acharya, P.; Acharya, S.; Minakawa, N.; Földesi, A.; Stoineva, I. B.; Yomtova, V. M.; Roussev, C. D.; Matsuda, A.; Chattopadhyaya, J.; Petkov, D. D. *ChemBioChem* **2005**, *6*, 992–996.

(12) Rangelov, M. A.; Vayssilov, G. N.; Yomtova, V. M.; Petkov, D. D. *Org. Biomol. Chem.* **2005**, *3*, 737–744.

(13) Rangelov, M. A.; Vayssilov, G. N.; Yomtova, V. M.; Petkov, D. D. *J. Am. Chem. Soc.* **2006**, *128*, 4964–4965.

(14) Wallin, G.; Åqvist, J. *Proc. Natl. Acad. Sci. U. S. A.* **2010**, *107*, 1888–1893.

(15) Sievers, A.; Beringer, M.; Rodnina, M. V.; Wolfenden, R. *Proc. Natl. Acad. Sci. U. S. A.* **2004**, *101*, 7897–7901.

SCHEME 1. Proposed Mechanisms for the Ammonolysis of Formyl-1,2-ethanediol via Tetragonal and Hexagonal Transition States (a) and Notation of the Atoms in the Modeled System on the Example of the Tetrahedral Intermediate I (b)

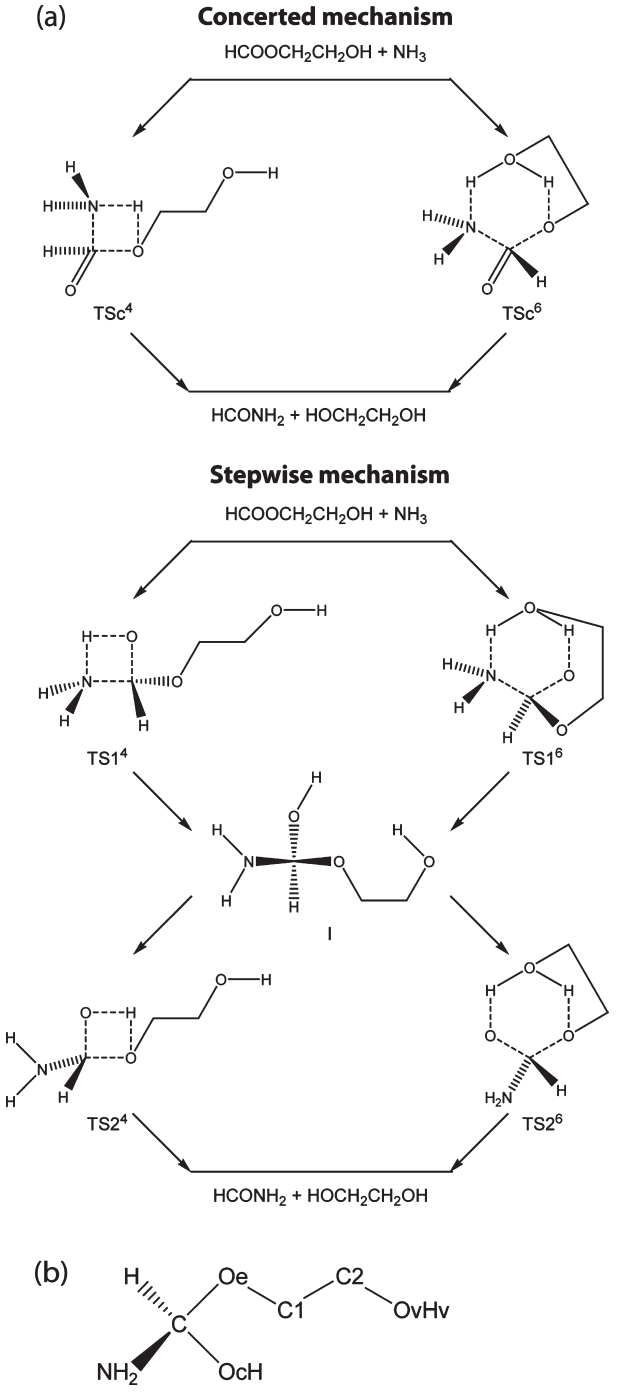

Our search for possible transition states and intermediates during the ammonolysis of monoacylated ethanediol suggested that the vicinal hydroxyl group could influence the reaction mechanism of the studied processes in two different ways: (i) by formation of intramolecular hydrogen bonds with the transition states and intermediates during the reaction resulting in the stabilization of the observed structures; (ii) by participation in the proton transfer (proton shuttle) both as proton donor and acceptor. In the first case the overall reaction path and topology of the transition states are not changed as compared to the noncatalyzed reaction, and the transition states remain tetragonal.

The active participation of the vicinal hydroxyl group in the proton transfer results in formation of a hexagonal TS cycle in which the bond breaking and forming occur due to participation of both Ov and Hv atoms of the vicinal hydroxyl in the elementary act. In both types of catalytic activation via vicinal OH group the intermediate I formed during the stepwise reaction path is the same (Scheme 1); that is, each of the transition states TS1 and TS2 could be either tetragonal or hexagonal (the type of reaction cycle is denoted as superscript). Obviously, the formation of hexagonal transition states is not possible for substrates lacking a vicinal OH group. However, such a role could be played by additional proton-donating and proton-accepting molecules (e.g., water, ammonia, alcohols, etc.) also acting as proton shuttle catalysts.[8a,9] For this reason, we also considered the catalytic influence of an external water molecule as a referent reaction.

The discussion of the different structures below uses the calculated electronic energies relative to the prereaction complex of 1-*O*-formyl-1,2-ethanediol and ammonia, while the analysis of the energetics of the reaction paths for different mechanisms is based on the corresponding Gibbs free energy values.

Catalytic Activation by a Hydrogen Bond from the Vicinal Hydroxyl (Tetragonal Transition States). Concerted Mechanism. The search for transition-state structures with intramolecular hydrogen bonds resulted in six distinguishable structures of TSc^4 with energy lower than that of the referent transition-state structure without a hydrogen bond shown in Figure 1 as filled black symbols and a black bar at the ordinate, respectively. In the different structures we found three types of hydrogen bonds: (i) HB(Oc−Hv) between the carbonyl Oc and the Hv atom from vicinal hydroxyl group (squares); (ii) HB(Ov−Ha) between Ov of the vicinal hydroxyl and one Ha atom from ammonia (diamonds); and (iii) HB(Oe−Hv) between the ester Oe atom and the proton from the vicinal hydroxyl Hv (triangles). In the figure we plotted the relative energy of the modeled transition states against the hydrogen bond length calculated as the distance between either the proton and the proton-acceptor center (a and c) or the proton-donor and proton-acceptor atoms (b and d).

The three couples of conformations differ mainly in the position of the C2 atom relative to the plane defined by the Oe, C1, and Ov atoms. For the structures with intramolecular hydrogen bonds the energy of the structure was found to depend on the proton transfer angle. The average proton transfer angle was estimated to be $125.6 \pm 1.9°$, much smaller than the optimal one of 180°. The first type of hydrogen bonds, HB(Oc−Hv), slightly shorter than the other types, was found in the most stable structure of TSc^4. This structure has also an additional HB between an ammonia hydrogen and Ov and is 7.7 kcal/mol more stable than the referent structure of TSc^4 without hydrogen bonds.

Stepwise Mechanism. For the first transition state of the stepwise mechanism, $TS1^4$, we found the same three types of hydrogen bonds already observed in the TSc^4 states: (i) Oc−Hv, (ii) Ov−Ha, and (iii) Oe−Hv. As could be expected, all obtained geometries with a hydrogen bond are more stable than the corresponding referent structures without a

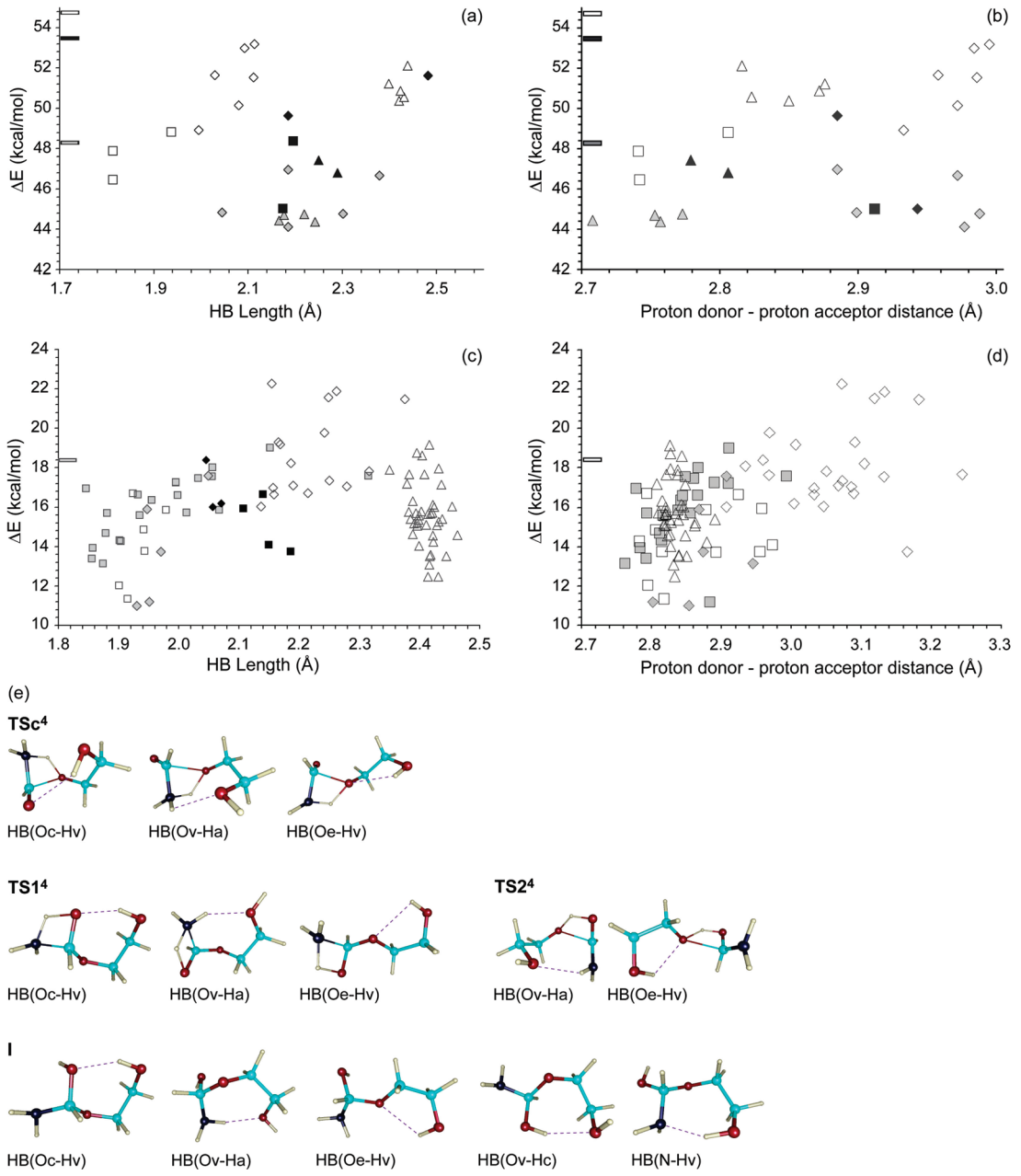

FIGURE 1. Relative energy of the various structures of the modeled tetragonal transition states (panels a and b) and intermediate (panels c and d) versus the length of the formed intramolecular hydrogen bond measured as the distance between the proton and the proton-acceptor center (panels a and c) or the distance between proton-donor and proton-acceptor atoms (panels b and d). Black, white, and gray colors of the symbols in panels (a) and (b) correspond to TSc^4, $TS1^4$, and $TS2^4$ transition state structures, respectively. The type of hydrogen bond is denoted as follows: Oc−Hv, squares; Ov−Ha, diamonds; Oe−Hv, triangles. The energy of the corresponding referent structures without a hydrogen bond is represented by bold bars on the ordinate axis. The type of hydrogen bond in the intermediate in panels (c) and (d) is denoted as follows: Oc−Hv, white squares; Ov−Ha, white diamonds; Oe−Hv, white triangles; Ov−Hc, gray squares; N−Hv, gray diamonds; the black symbols are applied for structures with more than one hydrogen bond. The energy of the referent structures without a hydrogen bond is represented by a bold bar on the ordinate axis. The reported energies are obtained at the B3LYP/6-31+G* level. (e) Examples of different types of hydrogen bonds in the transition states and the intermediate (color coding H, white; C, light blue; O, red; N, dark blue).

hydrogen bond (see Figure 1a,b; white symbols and white bar on the ordinate, respectively).

Similarly, the shortest hydrogen bonds are observed in the first type of structures with HB(Oc−Hv) as the average energy is estimated as 47.7 kcal/mol, and the structures are 7.0 kcal/mol more stable than the referent structure.

More than 70 stable conformations of intermediate I formed after $TS1^4$ along the stepwise reaction path were found. The large number of conformers is determined by the presence of three groups, NH_2, OvHv, and OcHc, that can form hydrogen bonds both as proton donors and proton acceptors. In addition, the Oe atom can act as a proton acceptor; that is, in total nine types of HB could be formed. However, four of these hydrogen bonds (N−Hc, Oc−Ha, Oe−Ha, and Oe−Hc) could be realized only via a four-membered cycle, which is disfavored as compared to five-membered cycles. On the other hand,

the vicinal OH group due to its distant location from the reaction centers forms large hydrogen-bonded cycles and takes part in the five remaining types of HB, observed in the stable structures of the intermediate. The influence of the hydrogen bond length on the stability of the modeled structures is presented in Figure 1c,d.

The structures with hydrogen bonds including the two hydroxyl groups, OcHc and OvHv, display the shortest hydrogen bonds in the intermediate with bond lengths of ca. 1.9 Å (Figure 1c) or 2.8 Å (Figure 1d), estimated as the distance between the proton acceptor and the proton or the proton donor. While the structures with OcHc as proton donor have a shorter HB, the structures with the reverse type of HB, i.e., with Oc as proton acceptor, have lower energy. The conformations with a HB between the N atom of the amino group as proton acceptor and the vicinal OH group as proton donor also have low energy, while the structures with reversed proton donor/acceptor are the least stable among all modeled intermediate structures. This is not surprising considering the relatively high basicity of the NH_2 group and the relatively high acidity of the OH group.

Similarly to TSc[4] and TS1[4], the formation of intramolecular hydrogen bonds results in stabilization of the second transition state, TS2, of the stepwise mechanism compared to the referent structure without a hydrogen bond (Figure 1a; gray symbols). Most of the observed structures with a HB have very similar energies, around 44 ± 2 kcal/mol. Unlike TSc and TS1 transition states, in this case only the last two types of hydrogen bonds are found: HB(Ov−Ha) (ii, diamonds) and HB(Oe−Hv) (iii, triangles). The HB(Oe−Hv) bonds have average energy of ca. 45.5 kcal/mol. The most stable structure among these conformers features the largest proton transfer angle, 130°.

Influence of the Orientation of the Hydrogen Bond. Since the structures containing an Oc−Hv hydrogen bond with vicinal OH as proton donor were found to be the most stable among the different modeled forms of the two rate-determining transition states TSc[4] and TS1[4], it could be instructive to estimate the influence of the hydrogen bond orientation on the stability of the two transition structures. For this reason, we studied the strength of the hydrogen bond formed between a water molecule and the Oc center of the TSc[4] and TS1[4] transition states for formic acid ammonolysis. The analysis is performed via stepwise variation of the valence angle C−Oc−Hw (Hw from the water molecule, participating in the hydrogen bond), denoted as A, and the dihedral angle D between the planes formed by C, Oc, and Hw, on one hand, and C, Oc, and N atoms, on the other (see left-hand part of Figure 2). The variation of the chosen angles is schematically presented in Figure S1 of the Supporting Information. In the applied procedure only the direction of the O−Hw bond in the water molecule is kept fixed, while the normal coordinates of the water molecule as well as the positions of the other atoms in the H_2O molecule relative to the transition-state structure are optimized. The obtained results are summarized in Figure 2 (a and b panels correspond to TSc[4] and TS1[4], respectively), representing the potential energy surface (PES) slice versus the two angles A and D.

According to the results obtained, the stabilization of TSc[4] resulting from the formation of a hydrogen bond with the Oc atom is ca. 5 kcal/mol for a large range of angles A and D. On the other hand, the hydrogen bond is most effective at angles

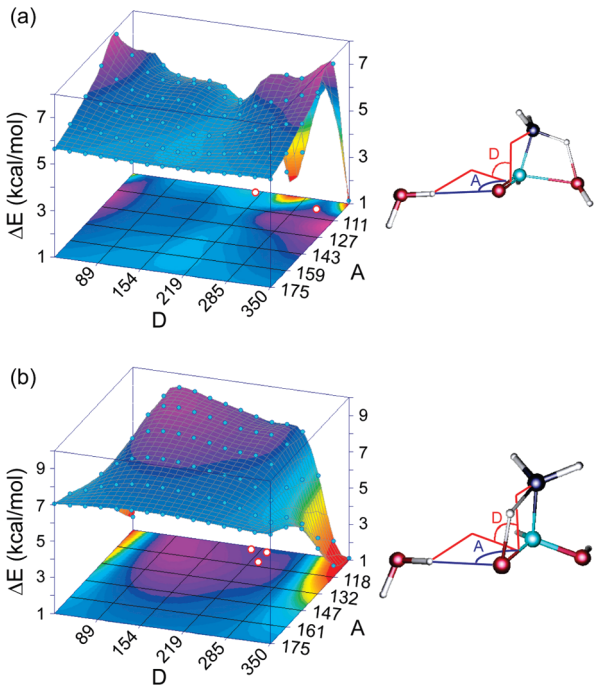

FIGURE 2. PES slice representing the influence of a water molecule on the stability of transition states TSc[4] (a) and TS1[4] (b) in the ammonolysis of formic acid. The blue points depict calculated values for the stabilization energy, while the white points represent the structures with minimal energy for formylethanediol as substrate. Definitions of angles A and D are shown on the right.

A = 120 ± 10° and D = 0 ± 10°, resulting in a decrease of the energy of the structure by 8 kcal/mol. The stabilization could be explained by the formation of an additional hydrogen bond between the Ha atom from the ammonia molecule and the oxygen atom Ow in the water molecule, and the contribution of such an additional hydrogen bond is roughly estimated to be 2−3 kcal/mol (Figure 2).

As discussed above, a similar effect was indeed observed in the case of the most stable structure of TSc[4] during ammonolysis of formylethanediol in which the formation of the two hydrogen bonds Oc−Hc and Ov−Ha results in stabilization of the transition state by 7.7 kcal/mol compared to the referent structure. The angles A and D (notation in Figure 2) for the most stable structure of the transition state TSc[4] in the ammonolysis process of formylethanediol are estimated to be A = 104.3° and D = −47.1°, i.e., close to the optimal values since the mobility of the vicinal OH group as related to the reaction center is limited by the covalent bonds.

The stabilization of the TS1[4] (Figure 2b) is estimated to be about 7 kcal/mol for a wide range of values of the angles A and D, while the maximal stabilization that can be achieved via the hydrogen bond is 9.5 kcal/mol for the optimal values of the angles A and D of 106° and 100°, respectively. The corresponding TS1[4] structures for formylethanediol with lowest energy (see the white circles on the projected PES plot) are characterized by almost optimal values of the valence angle A, around 110°, but the dihedral angle D, around 220°, differs considerably from the optimal one. The optimal value of the latter angle cannot be achieved since the position of the vicinal OH group in the ethanediol system is at the reverse side of the plane, defined by the atoms participating in the proton transfer process. The stabilization

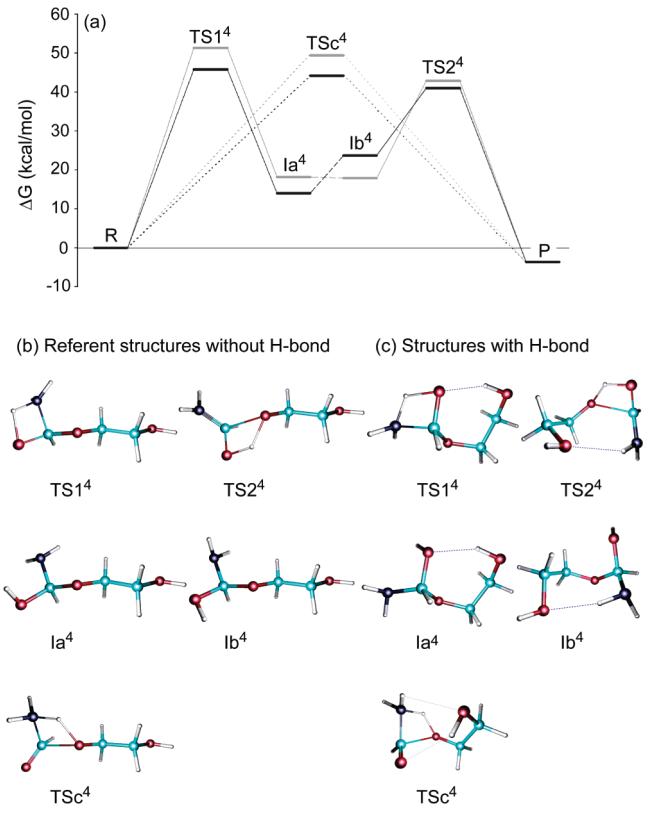

FIGURE 3. Gibbs free energy profile (at 298 K) of the ammonolysis reaction with tetragonal transition states. The energies of the referent structures without hydrogen bonds (with vicinal hydroxyl in *trans* position relative to the ether oxygen atom) are represented in dark gray. The energies of the lowest energy transition states with hydrogen bonds are represented in black. The stepwise mechanism is depicted with a solid line and the concerted one is depicted with a dotted line. The dashed lines in the stepwise reaction path represent sections where rotational barriers are located. The structures of the lowest energy transition states and corresponding intermediates are shown in panels (b) and (c).

of the most stable $TS1^4$ structure for the ethanediol model due to the hydrogen bond amounts to 7.8 kcal/mol.

Gibbs Free Energy Profile. The free energy profiles of the concerted and stepwise mechanisms for the ammonolysis of monoacylated ethanediol are presented in Figure 3, only the most stable structures of the tetragonal transition states with hydrogen bonds being included. For comparison, the optimized referent structures without hydrogen bonds (with the vicinal hydroxyl group in the *anti* position to the ether oxygen atom) are also shown. For the intermediate I we included two structures: the structure that is produced from the most stable structure of the TS1, and the structure from which the most stable conformation of TS2 is obtained.

If we consider the referent reaction path of ammonolysis of the conformer with the *anti*-oriented 2-OH group, i.e., without intramolecular hydrogen bonds, the reaction is found to be slightly exogonic, by 3.7 kcal/mol (Table 1). The concerted and the stepwise mechanisms have very similar free energies of activation, $\Delta G^{\#}$ (49.4 and 51.3 kcal/mol, respectively), as previously calculated for the aminolysis of 2-deoxyesters. This suggests that the *anti*-oriented 2-OH does not affect the mechanism of alkyl ester aminolysis

TABLE 1. Energy Values, Electronic Energy ΔE, and Gibbs Free Energy ΔG (both in kcal/mol) of the Transition States, Intermediate, and Product Calculated with Respect to the Initial State[a]

energy[b]	TSc	TS1	I1	I2	TS2	product[c]
ΔE(ref)	51.5	52.7	16.6	16.1	45.2	−4.5
ΔE(TG)	43.8	44.9	9.9	20.5	41.2	−4.5
ΔE(HG)	49.3	31.2	10.0	15.1	40.3	−4.5
ΔE(wat)	38.6	27.9	8.0	11.2	11.6	−2.9
ΔG(ref)	49.4	51.3	18.2	18.0	42.9	−3.7
ΔG(TG)	44.3	45.9	14.0	23.7	41.0	−3.7
ΔG(HG)	48.9	33.5	15.4	18.7	39.3	−3.7
ΔG(wat)[d]	38.9	30.0	13.0	14.9	29.5	−3.6
ΔG_{solv}(ref)	−7.2	−7.9	−1.9	−1.9	−3.4	−0.3
ΔG_{solv}(TG)	−3.9	−6.1	−2.4	−0.5	−2.1	−0.3
ΔG_{solv}(HG)	−0.9	−5.0	−2.4	−0.5	−0.9	−0.3
ΔG_{solv}(wat)	−7.9	−8.0	−2.7	−2.0	−4.3	−3.8
CCSD(T)						
ΔE(ref)	55.0	54.1	13.4	13.2	49.5	−3.1
ΔE(TG)	45.6	45.3	6.9	16.1	44.1	−3.1
ΔE(HG)	52.2	32.2	6.5	11.5	44.0	−3.1

[a]Calculations are performed at the B3LYP/6-31++G** level. In addition the Gibbs free energies of solvation, ΔG_{solv} (relative to the reactants), in acetonitrile and the values of the electronic energies obtained at the CCSD(T)/6-311++G**//MP2/6-311++G** level are reported. [b]The type of transition state is denoted in parentheses: ref: referent reaction; TG: tetragonal transition states; HG: hexagonal transition states; wat: reaction catalyzed by water. Only the energy of the most stable structures of each species is reported. [c]The reported energy values correspond to a complex formed by the species produced during the reaction. [d]The reported Gibbs free energy values are calculated relative to a prereaction complex including reactants and a water molecule as catalyst; taking into consideration the entropy contribution of the free water molecule before formation of the prereaction complex leads to an increase of all reported values by 3.0 kcal/mol.

due to its induction influence. The concerted transition state TSc^4 is found to be 1.1 kcal/mol more stable than the rate-determining TS1 of the stepwise mechanism.

Formation of hydrogen bonds with the vicinal OH group stabilizes the transitions states TSc^4 and $TS1^4$ by 5.2 and 5.5 kcal/mol, respectively; that is, the free energy of activation $\Delta G^{\#}$ of the reaction is reduced to 44.3 kcal/mol and the difference between the energy barriers for the concerted and the stepwise mechanisms remains only 1.6 kcal/mol. Despite some minor variations in the Gibbs free energies of the intermediate and $TS2^4$ due to formation of hydrogen bonds, the first step of the stepwise mechanism remains rate-determining.

In order to check for the influence of the computational level, we reoptimized the structures of the stationary points along the reaction path at the MP2 level and calculated the electronic energies of the species with the CCSD(T) method (Table 1). The higher-level computational method resulted in a small increase of the energies of all transition states by 0.3 to 4.3 kcal/mol, and the conclusions from the density functional calculations reported above are not altered.

Vicinal Hydroxyl As Proton Transfer Mediator (Hexagonal Transition States). In addition to the stabilization of the transition state via hydrogen bonds reported above, we also considered the vicinal OH group as a proton shuttle mediator in the aminolysis process as both proton donor and acceptor. Unlike the tetragonal transition states, a hexagonal cycle for the proton transfer is formed in these transition states (see right-hand side of Scheme 1a). The requirement for formation of a larger cycle in the transition state reduces the steric constraints in the structure and leads to a wider and thus more favorable angle for proton transfer. Since the vicinal hydroxyl group participates in the proton transfer,

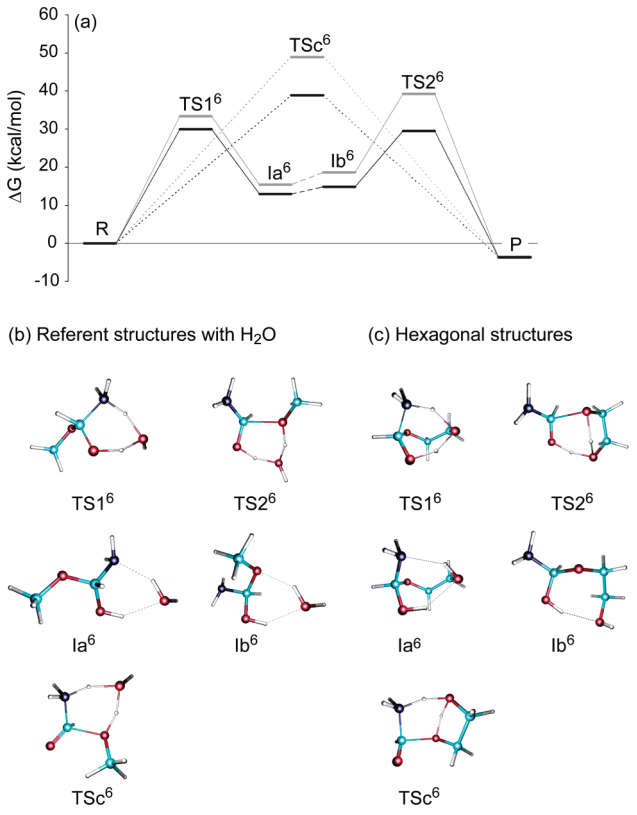

FIGURE 4. Gibbs free energy profile (at 298 K) for the ammonolysis of formyl-1,2-ethanediol via hexagonal transition states (in gray). Stepwise mechanism: solid line. Concerted mechanism: dotted line. The referent reaction of methyl formate ammonolysis, assisted by a water molecule, is shown with a black solid line. Dashed lines represent sections where rotational barriers are located. The structures of the lowest energy transition states and corresponding intermediates are shown in panels (b) and (c).

additional hydrogen bonds cannot be formed in the transition states and the conformational freedom is rather restricted.

A hexagonal structure of the transition states was already modeled in the case of ester ammonolysis catalyzed by different additional molecules that facilitate proton transfer.[7a,8,10] In this connection, as a referent system for the hexagonal transition states we modeled the ammonolysis of methyl formate catalyzed by a free water molecule instead of the vicinal OH group as a proton-mediating moiety (see Figure 4 and Gibbs Free Energy Profile section). Such a model allows us to evaluate the influence of the conformational constraints of the ethanediol moiety and the geometry restrictions of the vicinal OH group (in particular its position relative to the reaction center) on the energy of the transition states.

Both the concerted and stepwise mechanisms for ammonolysis of monoacylated ethanediol could occur via hexagonal transition states. The transition state TSc^6 of the concerted mechanism includes nucleophilic attack of the N atom to the carbonyl carbon atom and simultaneous proton transfers from the ammonia moiety to the vicinal hydroxyl and from the vicinal hydroxyl to the ester oxygen atom, Oe. The transfer of two protons is accomplished via hexagonal cycle. However, one of them, Hv, is transferred from Ov to the Oe center and participates in a pentagonal cycle as well. In addition to the restrictions from the smaller ring, the proton transfer between the vicinal oxygen atoms requires an unfavorable eclipsed conformation of ethanediol. For the transition state TSc^6 we found two conformations of the ethanediol moiety with similar energy. In both structures the cleavage and formation of the bonds between the heavy atoms is in a more advanced stage than the proton transfers.

The stepwise mechanism (Scheme 1a) includes formation of the same intermediate I as in the case of the tetragonal transition states. However, the transition state $TS1^6$, leading to this intermediate, differs from $TS1^4$. In $TS1^6$ the Ha proton from the ammonia moiety is not transferred directly to the Oc atom, as in $TS1^4$, but to the vicinal OvHv group, resulting in simultaneous migration of the proton Hv to the Oc atom. The second hexagonal transition state, $TS2^6$, besides cleavage of the C−Oe bond includes simultaneous proton transfer from the OcH group of the intermediate I to the Ov atom of the vicinal hydroxyl and from the vicinal hydroxyl to the ester oxygen atom, Oe. So, in both transition states the vicinal hydroxyl mediates the proton transfer.

Similarly to TSc^6, depending on the conformation of the ethanediol fragment, two conformations have been found for both hexagonal transition states of the stepwise mechanism $TS1^6$ and $TS2^6$. The structure of $TS2^6$ requires formation of an additional pentagonal cycle for the proton transfer of Hv, again similar to TSc^6. On the other hand, the second cycle for $TS1^6$ is larger, heptagonal, and has lower steric restrictions, which allow formation of the more favorable *gauche* conformation of the ethanediol moiety.

Gibbs Free Energy Profile. The reaction paths via hexagonal transition states for the studied and the referent systems are presented in Figure 4. The participation of the vicinal hydroxyl (or water molecule in the referent reaction) in the proton transfer cycle during the ammonolysis considerably changes the reaction energy profile compared to the noncatalyzed reaction. As can be seen, the stepwise mechanism becomes the lower energy path for the monoacylated ethanediol ammonolysis with a free energy barrier 15.5 kcal/mol lower than that of the concerted mechanism. While the Gibbs free energy of transition state $TS1^6$ in the stepwise mechanism is 5.8 kcal/mol lower than the second one ($TS2^6$), the first energy barrier is 12.9 kcal/mol higher than the second one due to the rather high energy of the intermediate. Thus, the free energy barrier of the reaction path via hexagonal transition states is 33.5 kcal/mol, 10.8 kcal/mol lower than that for the tetragonal TS structures.

Comparing the free energy barriers of the individual hexagonal transition states of the concerted mechanism with those calculated for the tetragonal transition states, one finds that the tetragonal transition state TSc^4 with a hydrogen bond is 4.7 kcal/mol more stable than the hexagonal one, TSc^6. The high energy of the latter structure is probably due to constraints caused by formation of the pentagonal ring and the unfavorable conformation of the ethanediol moiety discussed above. For the same reason the hexagonal form of the second transition state of the stepwise mechanism, $TS2^6$, is stabilized by 1.7 kcal/mol only as compared to the tetragonal one, $TS2^4$. The main advantage of the hexagonal transition state concerns the first transition state of the stepwise mechanism, which is stabilized by 17.9 kcal/mol relative to the corresponding most stable conformer of $TS1^4$.

In the referent reaction paths, where the proton transfer is carried out with the help of a water molecule, all structures

have lower energy as compared to the structures with proton transfer helped by the vicinal hydroxyl group. This energy difference of the corresponding transition states could be used for evaluation of the influence of steric constraints on TSc[6], TS1[6], and TS2[6]. The decrease of the TS1[6] barrier in the case of water-catalyzed ammonolysis is rather small, 3.5 kcal/mol, which implies a weak effect of the steric constraints in this transition state. Indeed, TS1[6] requires the formation of two unconstrained hexagonal and heptagonal cycles. The stabilization of the other two transition states, TSc[6] and TS2[6], is much stronger, by 10.0 and 9.8 kcal/mol, respectively. The comparable stabilization of these two transition states reflects their similar structure in the case of reaction with a monoacylated diol, which requires formation of a sterically constrained pentagonal cycle where the transfer of a proton between the two vicinal oxygen atoms of the diol (Ov and Oe) takes place. In addition, the covalent bonds in the ethanediol moiety fix the distance between Ov and Oe atoms participating in the proton transfer.

Similarly to the tetragonal transition states, the calculations with the CCSD(T)//MP2 approach (Table 1) lead to slight destabilization of the transition states by 1.2−4.1 kcal/mol. Thus, the reaction path with the hexagonal transition states occurs preferably via a stepwise mechanism, as we already concluded from the DFT results.

If we extend the interpretation of the computational results for catalysis by an additional water molecule to the process inside the ribosome, we have to take into account the difference in the entropy contributions of all components participating in the reaction step. In the real process the reaction occurs between two amino acid residues (represented in our model by ammonia and acylated ethanediol), each of them bound via covalent bonds to tRNA and with no separate translational and rotational entropy components. If catalysis is accomplished by the vicinal OH group, it is also part of the tRNA; that is, the translational and rotational entropy of the catalyst have no separate contributions. On the other hand, if one considers the additional water molecule as a catalytic species, then the entropy loss from its free state into a fixed position in the transition states should be taken into account. The evaluation of the translational and rotational entropy contribution of a free water molecule results in 14 kcal/mol at 310 K (corresponding to the ΔG value of a free water molecule). When the molecule is coordinated to the reaction center, this entropy loss is partially compensated by the enthalpy gain due to formation of hydrogen bonds. Our estimation for the change in ΔG from free to coordinated water is 3.0 kcal/mol; that is, the process is slightly endergonic and the prereaction complex is less stable than the system with free water. As described in the Computational Details the coordinated state of water is used as the initial state for calculation of the free energy profile of the reaction, shown in Figure 4 and reported in Table 1. Thus, in order to compare adequately the two alternative catalytic species, vicinal OH and additional water, we have to add 3.0 kcal/mol to the calculated $\Delta G^{\#}$ values of the transition states in the case of water. In this way the calculated free energy of the rate-determining transition state, TS1[6], for catalysis by an additional water molecule will be essentially equal to that of the corresponding transition state for the catalysis by the vicinal OH. The same approach could be followed in the analysis of the results of other model studies considering the catalytic effect from additional water (or another small molecule).

Reaction Path with Acetylated Vicinal Hydroxyl. In order to estimate the influence of a substituent at the carbonyl carbon atom, we calculated the reaction path via the tetragonal and hexagonal transition states for monoacetylated ethanediol as well. The structures corresponding to the various stationary points along the reaction paths were optimized starting from the structures of the formylated reactant with the methyl group at the position of the H atom bound to the carbonyl C atom. In all cases the calculated Gibbs free energies of the transition states are higher than the corresponding structures for ammonolysis of formylethanediol (see Figure S2 in the Supporting Information). The increase is similar for the tetragonal and the hexagonal transition states: 2.7, 4.9, and 2.7 kcal/mol for TSc[4], TS1[4], and TS2[4] and 3.0, 3.5, and 4.6 kcal/mol for TSc[6], TS1[6], and TS2[6]. Since the changes are synchronous, the presence of the additional methyl group does not affect the preferred reaction mechanism, but the Gibbs free energy of activation of the process increases to 37.0 kcal/mol.

Evaluation of the Influence of the Environment on the Gibbs Free Energies. Since the environment of the reaction center both in aprotic solvents and inside the ribosome is different from vacuum, we evaluated the influence of the surroundings of the reaction center on the reaction energetics by calculation of the free Gibbs energies of solvation for all stationary points along the modeled reaction paths. This approach accounts for the nonspecific interactions of the dielectric medium with the reactants, transition states, and intermediates. For the calculations we selected three solvents with different dielectric constants: chloroform with $\varepsilon = 4.71$, acetonitrile with $\varepsilon = 35.69$, and "water" with $\varepsilon = 78.35$ (note that only electrostatic and dispersion interactions are taken into account, while the specific interactions such as formation of hydrogen bonds or proton transfer are not considered in this approach).

Solvation was found to stabilize all transition states, as the stabilization of certain species increases with the dielectric constant of the solvent (see Figures S5−7 of the Supporting Information). Accounting for the polarization of the surroundings, however, does not result in qualitative alteration of the preferred reaction mechanism, and the energetically most favorable route is via hexagonal transition states. The reduction of the Gibbs free energy barriers of the referent reaction path without formation of a hydrogen bond and via tetragonal transition states due to solvation is 7.2 and 3.9 kcal/mol, respectively, as can be seen from Table 1, where the calculated ΔG_{solv} values for acetonitrile as solvent are shown. The influence of the medium was most pronounced for transition state TS1 in all modeled reaction paths. In particular, for the most preferable reaction path via the hexagonal transition states the Gibbs free energy barrier is reduced due to the effect of the surroundings by 3.8, 5.0, and 5.3 kcal/mol for chloroform, acetonitrile, and water; that is, for a medium with ε around 35 the reaction barrier is reduced from 33.5 kcal/mol under vacuum to 28.5 kcal/mol.

Conclusions

The present computational model study evaluates the influence of the vicinal OH group in acylated diols on the reaction paths for ester ammonolysis. Two alternative

approaches for this influence were considered: stabilization of the (tetragonal) transition states along the reaction path via hydrogen bonds and participation of the vicinal hydroxyl in proton transfer (proton shuttle mechanism).

The catalytic activation of the ester ammonolysis by a hydrogen bond from the vicinal hydroxyl via tetragonal transition states (occurring preferably via a concerted mechanism) was found to be rather modest, the free energy of activation being reduced by 5.2 kcal/mol only. The resulting free energy of activation, $\Delta G^{\#} = 44.3$ kcal/mol, is still rather high, and for this reason the pathway via tetragonal transition states is unlikely to occur. The reason for this weak catalytic effect is the rather small proton transfer angles in the transition states, about 125−130°, much smaller than the optimal angle of 180°. The comparison with stabilization of the transition states via a hydrogen bond from an external water molecule suggests that the stabilization in the case of monoacylated ethanediol is close to the maximally possible stabilization of this type.

The other mechanism of catalytic activation of the ester ammonolysis—by participation of the vicinal hydroxyl in the proton transfer via hexagonal transition states—does not affect considerably the stability of the transition states in the concerted mechanism and the second step of the stepwise mechanism. However, it stabilizes considerably the first transition state of the stepwise mechanism; the Gibbs free energy of activation is reduced by 16.0 and 10.8 kcal/mol with respect to the referent value and the barrier for stabilization of the transition states via a hydrogen bond. The resulting free energy of activation, 33.5 kcal/mol, is significantly lower than the barriers calculated for the noncatalyzed reaction or the reaction occurring via the tetragonal transition states. The main reason for this effect[13] is the replacement of a single unfavorable proton transfer in TS1[4] by two favorable proton transfers in TS1[6] that decreases the angular distortions for the proton transfers, as can be concluded from the larger angles, 149° and 155°.

A similar catalytic effect has been proposed for water-assisted aminolysis of 2-deoxy esters,[9] where the OH group of water acts as a proton shuttle in the same way as the vicinal OH in monoacylated 1,2-ethanediol aminolysis modeled here. As we have shown, however, the proper accounting of the (translational and rotational) entropy of the free water molecule resulted in an increase of the free Gibbs energy of activation for the water-assisted process. Such entropy loss does not influence the free energy of the transition states in the case of catalysis by vicinal OH since the catalytic group is bound by a covalent bond to the reaction center. In addition, the vicinal 2′-OH of ribose, modeled here as ethanediol, is readily available, being next to the reaction center during the synthesis of each peptide bond. Catalysis including an additional water molecule would require the approach of an external water molecule to the reaction center to accomplish each reaction step. Thus, we consider the vicinal 2′-OH of the ribose as a realistic and relevant proton transfer mediator for the peptide bond formation in the ribosome. This conclusion is also supported by the lack of reactivity of the modified peptidyl tRNA in which A76 2′-OH was substituted by H, F, or a methoxy group.[2e,11] The 2′-OH keeps its catalytic activity even when embedded into an active site of six neighboring 2′-deoxyribose nucleosides.[16] In addition, the proton shuttle role of the 2′-OH corroborates the crystal structure analysis[17] and computational modeling.[2b]

In summary, the proton shuttle role of the vicinal OH was found to provide stronger activation of the reaction of peptide bond formation than the activation via an additional hydrogen bond from this group. The more favorable structure of the transition states for ester aminolysis due to participation of the vicinal hydroxyl in the proton transfer results in a decrease of the free energy of activation by 16.0 kcal/mol, which corresponds to about 10^9-fold acceleration of the reaction with respect to the noncatalyzed process. This value is in agreement with the lowest experimental estimate for acceleration of this process in the ribosome, 10^6-fold, reported by Weinger and Strobel.[18]

Accounting for the influence of the environment on the reaction center by a continuum model (for ε from 5 to 80) resulted in further stabilization of the rate-determining transition state by 4−5 kcal/mol.

As discussed in the present paper, the transformations in the reaction center during the elementary steps of the ester aminolysis catalyzed by the vicinal hydroxyl have two components: proton transfer and cleavage/formation of a bond between heavier atoms (C−O or C−N). We have shown that the transition-state energies are reduced when the structure of the reaction center allows formation of C−N or cleavage of C−O bonds together with favorable arrangement for simultaneous proton transfer. The proton transfer itself can be influenced also by other factors and processes, which have been extensively studied in connection with the importance of the proton transfer in enzymes, nucleic acids, and various other biochemical systems. Recently, Warshel and co-workers[19−22] have presented a series of studies with critical analysis of the different ideas on the proton transfer processes in enzymes. They have pointed out that the fluctuations of the polar environment, which modify the reaction barrier, are actually responsible for facilitation of the proton transfer and for the enormous catalytic power of enzymes in general. On the basis of the analysis of available experimental results and related computational modeling at the microscopic level, they have shown that the tunneling, as accounted for by the kinetic isotope effect, does not contribute significantly to the catalytic activity of the enzymes since similar effects occur in the referent noncatalyzed reactions in solution.[19,21] Taking into account the analogies in the catalysis by the enzymes and by the ribosome, one may assume that these features would also influence the proton transfer processes in the ribosome, as a component of the elementary reaction step for peptide bond formation.

(16) Erlacher, M. D.; Lang, K.; Wotzel, B.; Rieder, R.; Micura, R.; Polacek, N. *J. Am. Chem. Soc.* **2006**, *128*, 4453–4459.

(17) Schmeiling, T. M.; Huang, K. S.; Kitchen, D. E.; Strobel, S. A.; Steitz, T. A. *Mol. Cell* **2005**, *20*, 437–448.

(18) Weinger, J. S.; Strobel, S. A. *Blood Cells Mol., Dis.* **2007**, *38*, 110–116.

(19) Braun-Sand, S.; Olsson, M. H. M.; Mavri, J.; Warshel, A. In *Hydrogen Transfer Reactions*; Hynes, J. T.; Klinman, J. P.; Limbach, H.-H.; Schowen, R. L., Eds.; Wiley-VCH: Weinhein, 2007; pp 1171−1205.

(20) Warshel, A.; Sharma, P. K.; Kato, M.; Xiang, Y.; Liu, H.; Olsson, M. H. M. *Chem. Rev.* **2006**, *106*, 3210–3235.

(21) Kamerlin, S. C. L.; Mavri, J.; Warshel, A. *FEBS Lett.* **2010**, *584*, 2759–2766.

(22) Kamerlin, S. C. L.; Sharma, P. K.; Chu, Z. T.; Warshel, A. *Proc. Natl. Acad. Sci.* **2010**, *107*, 4075–4080.

Computational Details

All *ab initio* molecular orbital calculations were performed with the Gaussian03[23] program suite. Analytical gradient optimization methods were used to locate the minima, corresponding to reactants, intermediates, and products, and saddle points corresponding to transition states. Transition states were identified by finding only one negative eigenvalue of the analytic force constant matrix and by geometric analysis of its eigenvector components. All lowest points of reaction paths were optimized at the B3LYP/6-31++G** level,[24,25] and the electronic energies of the obtained structures were refined by single-point calculations with the high-level post-Hartree−Fock method CCSD(T) with the 6-311++G** basis set. The latter method allows avoiding the well-known "delocalization error" of modern density functional methods, which could result in an overstabilization of fractional charges and thus could affect the relative stability of the transition states.[26] In addition, we reoptimized the structures of the stationary points along the reaction path at the MP2/6-311++G** level starting from the structures optimized with the B3LYP/6-31++G** approach. Subsequently, the electronic energies of the structures were recalculated with the CCSD(T) method and the obtained CCSD(T)//MP2 energies are reported in Table 1. The energy difference between the CCSD(T)//B3LYP and CCSD(T)//MP2 methods for different stationary points was found to be at most 1.3 kcal/mol (0.5 kcal/mol on average).

The influence of the surroundings on the relative Gibbs free energies of the transition states was estimated as the solvent effect of solvents with different dielectric constants (from $\varepsilon = 4.71$ to $\varepsilon = 78.35$). The calculations were performed in single-point fashion (B3LYP/6-31++G** level) with the polarized continuum model.[27]

The energies of all structures within each reaction path are calculated with respect to the energy of the initial complex formed by the reactant molecules formyl-1,2-ethanediol and ammonia with two intramolecular hydrogen bonds (Ha−Oc and Hv−N). Thus, the energy of the complex formed by the product molecules is considered as the reaction energy. Since all species along each reaction path have the same composition, the correction for basis set superposition error is not calculated. The activation barriers of the transition states TS1 and TSc are considered with respect to the reactants, while the activation barriers of the second transition states TS2 are estimated with respect to the intermediate I, which is geometrically closest to TS2. The changes of the Gibbs free energy values ΔG of all stationary points along the reaction paths were also calculated with respect to the corresponding value of the reactants. For the reaction path with an additional water molecule as a catalyst participating in the proton transfer we also considered the translational and rotational entropy contribution of a free water molecule (corresponding to the ΔG value of the free water molecule). This is necessary for correct comparison of different reaction paths since all other components of the reaction are parts of large tRNA molecules, while only the water molecule is free.

A complete model study of the reaction mechanism and energetics requires a search not only of all possible intermediates and transition states along the different reaction paths but also of the different conformations of all stationary points along each reaction path in order to find those with lowest energy. For this reason, our investigation included a complete conformational search aiming at finding all lowest energy structures. The applied computational procedure, described in detail in ref 28, is based on the generation of a set of initial structures via stepwise variation of different dihedral angles (N−C−Oe−C1, C−Oe−C1−C2, Oe−C1−C2−Ov, and C1−C2−Ov−Hv) by 10°. Thus, about 46 000 to 160 000 initial structures were generated for each transition state and intermediate, which were further sifted out by elimination of equivalent structures.

The carbonyl carbon atom is prochiral, and after nucleophilic attack of ammonia a chiral intermediate is formed; that is, two reaction paths with *R* or *S* intermediates are possible. However, both reaction paths are energetically equivalent, and we consider only the pro *R* attack and *R* configuration of the intermediates.

Rotational barriers between the intermediates along the reaction paths were not calculated since these barriers are significantly lower than the transition states, and therefore they cannot influence the reaction kinetics (for more details see Figure S3 of the Supporting Information.

The dependence of the Gibbs free energy of activation for the different transition states on temperature was also studied (see Figure S4 of the Supporting Information. The analysis shows that the changes in the barriers of the studied reaction paths are synchronous for each group of transition structures, and variation of the temperature does not result in interchange of the rate-determining stages in the temperature range 293−333 K. One should note, however, that the variation of the temperature may strongly affect the fluctuations of the environment and thus influence the dynamics of the proton transfer reactions via modification of the energy barrier for the process, as concluded for proton transfer processes in enzymes.[19]

The following notation is applied for the stationary points along concerted and stepwise reaction pathways: TSc, transition state of concerted mechanism; TS1 and TS2, first and second transition states of the stepwise path; I, intermediate of the stepwise path. The superscript (4 or 6) denotes the number of atoms participating in the cycle of the corresponding transition states. The notation of atoms is represented in Scheme 1b with the example of the tetrahedral transition state, I, observed in the stepwise mechanisms of the reaction.

Acknowledgment. The authors are grateful to the National Research Fund of Bulgaria for financial support via Grant Nos. DO 02-133/2008, DO 02-210/2008, and the Center of Excellence for Supercomputer Applications DO

(23) Frisch, M. J.; Trucks, G. W.; Schlegel, H. B.; Scuseria, G. E.; Robb, M. A.; Cheeseman, J. R.; Montgomery, J. A., Jr.; Vreven, T.; Kudin, K. N.; Burant, J. C.; Millam, J. M.; Iyengar, S. S.; Tomasi, J.; Barone, V.; Mennucci, B.; Cossi, M.; Scalmani, G.; Rega, N.; Petersson, G. A.; Nakatsuji, H.; Hada, M.; Ehara, M.; Toyota, K.; Fukuda, R.; Hasegawa, J.; Ishida, M.; Nakajima, T. ; Honda, Y.; Kitao, O.; Nakai, H.; Klene, M.; Li, X.; Knox, J. E.; Hratchian, H. P.; Cross, J. B.; Bakken, V.; Adamo, C.; Jaramillo, J.; Gomperts, R.; Stratmann, R. E.; Yazyev, O.; Austin, A. J.; Cammi, R.; Pomelli, C.; Ochterski, J. W.; Ayala, P. Y.; Morokuma, K.; Voth, G. A.; Salvador, P.; Dannenberg, J. J.; Zakrzewski, V. G.; Dapprich, S.; Daniels, A. D.; Strain, M. C.; Farkas, O.; Malick, D. K.; Rabuck, A. D.; Raghavachari, K.; Foresman, J. B.; Ortiz, J. V.; Cui, Q.; Baboul, A. G.; Clifford, S.; Cioslowski, J.; Stefanov, B. B.; Liu, G.; Liashenko, A.; Piskorz, P.; Komaromi, I.; Martin, R. L.; Fox, D. J.; Keith, T.; Al-Laham, M. A.; Peng, C. Y.; Nanayakkara, A.; Challacombe, M.; Gill, P. M. W.; Johnson, B.; Chen, W.; Wong, M. W.; Gonzalez, C.; Pople, J. A. *Gaussian 03*, Revision E.01; Gaussian, Inc.: Wallingford, CT, 2004.

(24) (a) Ditchfield, R.; Hehre, W. J.; Pople, J. A. *J. Chem. Phys.* **1971**, *54*, 720–723. (b) Hehre, W. J.; Ditchfield, R.; Pople, J. A. *J. Chem. Phys.* **1972**, *56*, 2257–2261. (c) Hariharan, P. C.; Pople, J. A. *Mol. Phys.* **1974**, *27*, 209–214. (d) Gordon, M. S. *Chem. Phys. Lett.* **1980**, *76*, 163–168. (e) Hariharan, P. C.; Pople, J. A. *Theor. Chim. Acta* **1973**, *28*, 213–222.

(25) McLean, A. D.; Chandler, G. S. *J. Chem. Phys.* **1980**, *72*, 5639–5648.

(26) (a) Gritsenko, O. V.; Ensing, B.; Schipper, P. R. T.; Baerends, E. J. *J. Phys. Chem. A* **2000**, *104*, 8558–8565. (b) Mori-Sanchez, P.; Cohen, A. J.; Yang, W. T. *Phys. Rev. Lett.* **2008**, *100*, 146401.

(27) (a) Miertuš, S.; Scrocco, E.; Tomasi, J. *Chem. Phys.* **1981**, *55*, 117–129. (b) Miertuš, S.; Tomasi, J. *Chem. Phys.* **1982**, *65*, 239–245. (c) Tomasi, J.; Mennucci, B.; Cammi, R. *Chem. Rev.* **2005**, *105*, 2999–3094.

(28) Rangelov, M. A.; Petrova, G. P.; Yomtova, V. M.; Vayssilov, G. N. *J. Mol. Graphics Modell.* **2010**, *29*, 246−255.

02-115/08. This work is dedicated to the memory of Prof. D.Sc. Dimiter D. Petkov, who inspired and started it.

Supporting Information Available: Scheme of variation of the angles A and D used in evaluation of the influence of the orientation of the hydrogen bond; Gibbs free energy profile for the reaction path with acetylated vicinal hydroxyl; energy profile for rotation of different torsion angles in the intermediate I; temperature dependence of Gibbs free energy barriers; figures with Gibbs free energy profile of the reaction paths including solvation energy for different solvents; tables of atom coordinates and absolute energies of the stationary points along the modeled reaction paths. This material is available free of charge via the Internet at http://pubs.acs.org.